

Power-line Interference Elimination from ECG Signals Using Modified Notch Filtration: A Real Time Version

Georgy Mihov^{1*}, Ivan Dotsinsky²

¹Department of Electronics
Faculty of Electronic Engineering and Technologies
Technical University of Sofia
8 Kliment Ohridski Blv., Sofia 1000, Bulgaria
E-mail: gsm@tu-sofia.bg

²Institute of Biophysics and Biomedical Engineering
Bulgarian Academy of Sciences
Acad. Georgi Bonchev Str., Bl. 105, Sofia 1113, Bulgaria
E-mail: iadoc34@gmail.com

*Corresponding author

Received: May 14, 2025

Accepted: December 16, 2025

Published: March 31, 2026

Abstract: The traditional notch filtration (NF) seems to be appropriate for successfully suppressing the power-line interference (PLI) commonly encountered in electrocardiographic (ECG) recordings. However, this can be achieved by a very narrow bandwidth that does not correspond to the PLI variations inducing unacceptably long transition periods. The present study is based on previous works cited below, where the contaminated ECG recording is band-pass (BP) filtered, the introduced phase shift is compensated by a back filtration, and the ongoing first harmonic frequency is off-line determined by measuring the time between two consecutive zero-line crossings. The proposed in this paper methodology subjects the contaminated ECG recording to two-fold one-way BP filtration, the second one contributing to a more accurate first harmonic extraction. Further one, a more precise sinusoidal interpolation for zero-line crossing detection enables high fidelity calculation of the ongoing PLI first harmonic. The frequency deviation of the PLI is compensated by calculating the first derivative of the phase response of the two-fold BP filtration, and the amplitude variation of the PLI – by calculating the gain from the frequency response. The NF coefficients determined in this way are applied to the subsequent specific band-stop filtration of the ECG signals. Two additional problems are also studied and taken in consideration – the elimination of high-order harmonics in power-line interference and the procedure adaptation to low sampling rates. The experiments are carried out in MATLAB environment.

Keywords: ECG signals, Power line interference suppression, Unidirectional band pass filtration, Modified notch filtration, High harmonics.

Introduction

One of the main sources for degradation of the acquired electrocardiographic (ECG) signals is the power supply. The residual power-line interference (PLI) complicates the ECG signals analysis and embarrasses the correct diagnosis. Over the past few decades, numerous scientific studies have been devoted to methods, algorithms and techniques for synthesizing universal and specialized filters that reduce the PLI without introducing changes in the ECG signal shape.

Different types of notch filters have been developed. Dobrev et al. [2] use a simple digital approach to extract the PLI. The real and the imaginary parts of the disturbance are found by means of two digital mixers with rectangular or sinusoidal shape of the demodulated signal.

Then the PLI is synthesized and extracted. Typically, the notch comb filters affect the frequency components of the ECG around the rated PLI frequency. The simple band-pass (BP) filter presented by Neycheva et al. [14] is based on correlated averaging, leading to a comb frequency response. It has high Q-factor notches at odd harmonics of the power supply disturbances and is suitable for their suppression. Dobrev et al. [3] propose a linear-phase comb filter for PLI suppression, operating in parallel with a low-pass averaging filter to recover the filtered low-frequency components. A comb filter with high Q-factor notches is achieved for all harmonics of the mains frequency by correlated averaging of samples multiples of the PLI period and subsequent subtracting the result from the input signal. Non-adaptive high Q-factor notch filters can follow the PL frequency deviations allowed to a small extent by the standard [12].

Adaptive notch filters can significantly better suppress disturbances in the presence of non-stationary interference from the power supply with amplitude variation and rated frequency deviations. In Shaddeli et al. [17], an adaptive notch filtering of PLI based on the least-mean square (LMS) method is proposed. To improve the traditional LMS method, evolutionary algorithms are used to select the optimal variable LMS step size, causing the smallest error between the contaminated and filtered ECG signals. Ivanov et al. [10] present a strategy for training a deep convolutional autoencoder for removing PLI from ECG signals. The study uses 12-channel ECG recordings from the PhysioNet database contaminated by simulated sinusoidal PLI noise with increased parameters. The Adam optimizer and the Mean square error loss function are applied for training. The quality of the clean ECG reconstruction is evaluated by the root mean square error, percentage root-mean-square difference, and signal-to-noise ratio improvement.

High-frequency components of interest up to 1 KHz may be observed in ECG signals with high resolution and sampling rate together with traditional PLI and its harmonics. Badreldin et al. [1] propose a modified adaptive notch filter that suppresses the PLI harmonics without using an external reference signal from the power supply. The achieved suppression is comparable to that in idealized adaptive systems using an external reference signal. Razzaq et al. [15] published an intelligent adaptive filter to eliminate PLI, as well as its first, third and fifth harmonics, without any auxiliary reference input. The proposed system is based on the space state recursive least square (SSRLS) adaptive filter. In Ur-Rehman et al. [20], a parallel running of the state space recursive least square algorithm was introduced, which removes PLI together with its harmonics up to the 9-th with lower computational costs.

Other techniques applied to PLI suppression are the neural networks. Mateo et al. [13] propose suppression of the PLI fundamental harmonic, using an incremental artificial neural network adapted by an improved Widrow-Hoff Delta algorithm. In Rizanov and Mihov [16], a PLI suppression filter based on a genetic algorithm is presented, which does not require prior training of the machine learning model. Since the PLI first harmonic can be defined by a specific amplitude, frequency, and phase, the optimization path of the genetic algorithm finds a suitable sinusoid that is extracted from the contaminated ECG signal, thereby suppressing the mains interference.

Dotsinsky and Stoyanov [7] published an innovative method for software measurement of the PLI frequency. The contaminated signal is BP filtered from 49 to 51 Hz. The amplitudes of two adjacent samples on a positive-going slope of the mains interference, located below and above the zero line, are measured, and by linear interpolation of the crossing point, the ongoing PLI period is estimated. The software measurement of the PLI frequency is the basis of the

proposed procedure in Dotsinsky [4], and Dotsinsky and Stoyanov [7] for removing main interference in ECG, which is implemented in three stages. The first one resamples the contaminated signal so that the variable PLI frequency is transformed into a rated constant frequency. The second stage rejects the PLI, and the third one performs a back resampling to restore the normal time rate. For both re-samplings, experiments were performed with four-point and eight-point Lagrange polynomials, as well as with linear interpolation [4, 7]. For the second stage, a notch filter was used. In Dotsinsky [5], the method was applied with a larger frequency deviation from 12.5 to 18.8 Hz when filtering ECG signals recorded by public access defibrillators in the presence of railway AC power interference with a frequency of 16.7 Hz. A comb filter was chosen as more suitable for the case for rejecting interference in the second stage. An adaptive filter for mains interference suppression is presented in Stoyanov et al. [19]. The filter is automatically switching between 50 and 60 Hz processing, using two parallel operating BP filters. The PLI frequency is measured by zero-line crossing detection, followed by more precise localization applying Lagrange interpolation, then suppressed by an adaptive LMS algorithm using reference signals from previously prepared tables.

The method for software measurement of the PLI frequency [7] was improved by Dotsinsky and Stoyanov [8]. The BP filtering was enlarged twice – from 48 to 52 Hz. The crossing point of the PLI with the zero line was determined using homogenous triangles formed by the four closest samples located below and above the zero line. As in [7], the elimination of PLI uses three stages, with the two re-samplings being performed with linear interpolation. Parallel experiments were carried out with a rejecting stage applying the subtraction method and a notch filter. It was found that the optimal option for PLI rejecting is the subtraction procedure, while a long-term absence of linear segments has to automatically introduce the notch filtration – these are typical cases for the beginning of fibrillation or ventricular tachycardia.

The subtraction procedure for mains interference eliminating from ECG signals Levkov et al. [11] was modified in Dotsinsky et al. [9], using some techniques from [7] to determine the crossing points of the ongoing PLI sinusoid with the zero line. The contaminated ECG signal is processed by a BP filter with a central frequency at 50 Hz and bandwidth from 48 to 52 Hz. The phase shift is zeroed by applying the same filter once more but backwards. The positions of the crossing points determined by linear interpolation are used to calculate a fractional number of samples in the ongoing PLI wave, leading to more accurate filtering by moving averaging.

Dotsinsky [6] published a successful notch filter providing almost complete elimination of Power Line Interference (PLI). The testing of the method and the evaluation of the obtained results were performed with authentic, conditionally clean ECG recordings, which were mixed with synthesized interference. The interference has a frequency of 50 Hz, which varies from 49 to 51 Hz within 20 s. As in [9], the PLI first harmonic is extracted from the contaminated signal by BP filtration with a center frequency $f_0 = 50$ Hz, with the left and right cutoff frequencies being $f_\ell = 48$ and $f_r = 52$ Hz, respectively. To avoid phase shift, BP filtration is bidirectional (Bidirectional – BP-filter is applied twice – first time in the “forward” direction, and second time – in the “backward” direction). Then, the individual length of each PLI sinusoid is calculated by measuring the distance T_i between two consecutive increasing crossings with the zero line (Fig. 1).

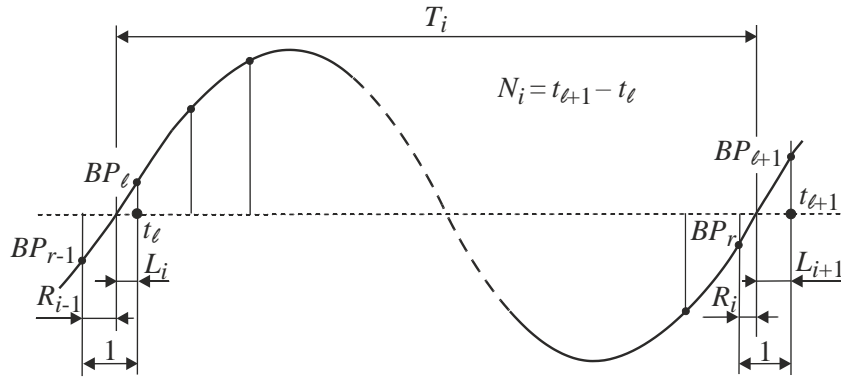


Fig. 1 Principle of determining the individual length of each PLI sinusoid (the figure is borrowed from [6])

The ongoing frequencies f_i of the first PLI harmonic are determined from the dependencies:

$$L_{i+1} = \frac{BP_{\ell+1}}{BP_{\ell+1} - BP_r}, \quad L_i = \frac{BP_\ell}{BP_\ell - BP_{r-1}}, \quad T_i = N_i - L_{i+1} + L_i, \quad f_i = \frac{Q}{T_i}. \quad (1)$$

Here and below Q states for the sampling rate. This is followed by notch filtration (NF) of the contaminated ECG signal, which is performed with recalculated coefficients at the ongoing frequency f_i determined by the BP filter and a twice narrower rejection band $(f_r - f_\ell)/2 = 2$ Hz. To compensate PLI amplitude variations, the NF filtration is bidirectional, with the notch filter applied twice – in the “forward” and “backward” directions. The application of bidirectional BP and NF filtration requires the entire PLI elimination procedure to be performed outside of real time. The stages of the procedure are five: ‘i’ – BP filter in the “forward” direction; ‘ii’ – BP filter in the “backward” direction; ‘iii’ – calculation of the coefficients for the NF filtration; ‘iv’ – NF filtration “forward”; ‘v’ – NF filtration “backward”.

Stoyanov et al. [18] published a modified version of [6], where the PLI elimination is performed sequentially on parts of the ECG signal with a duration of 1 s. This allows the filtration to be performed in quasi-real time. In addition, filtration of the third PLI harmonic $3 \times f_i$ is introduced, applying a one-way notch filter using the first PLI harmonic f_i , calculated from Eq. (1).

The present study aims to implement the proposed in [6] and improved in [18] PLI suppression procedure in full real time mode. For this purpose, it is necessary to replace the bidirectional filters with unidirectional ones. Additionally, the problems of applying the procedure at low sampling frequencies (less than 1 000 Hz) must be resolved together with the determination of the mains interference level, below which the PLI sinusoid length should not be calculated due to the generation of unrealistic values.

Materials and methods

The proposed PLI suppression is implemented in full real time mode in five stages as in [6] where the stages ‘ii’ and ‘v’ apply “forward” filtrations instead of “backward” ones.

Stages ‘i’ and ‘ii’ – band-pass filtration

The BP filter (Eq. (2)) is in the basis of the PLI elimination procedure in [6] and [18]. When applied twice in one direction, i.e., $\mathbf{H}_{PB}(z) \times \mathbf{H}_{PB}(z)$, the equivalent frequency and phase responses have the shape shown in Fig. 2.

$$\mathbf{H}_{\text{BP}}(z) = \frac{1-z^{-2}}{1-a_1z^{-1}+a_2z^{-2}} \cdot \frac{1-a_2}{2}, \quad \left| \begin{array}{l} a_1 = \frac{2 \cos \frac{2\pi f_0}{Q}}{k+1}, \quad k = \text{tg} \frac{\pi(f_r - f_l)}{Q} \\ a_2 = \frac{1-k}{1+k} \end{array} \right. \quad (2)$$

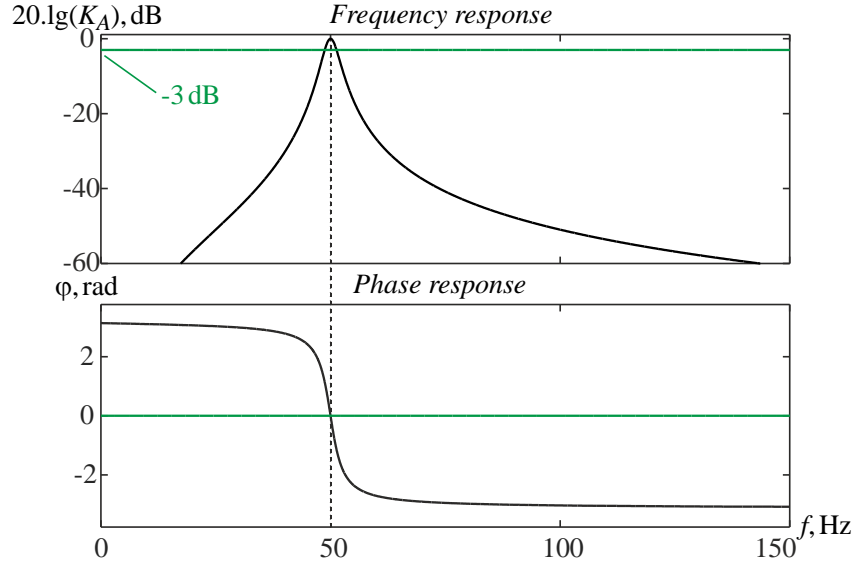


Fig. 2 Responses of the twice applied BP filter $\mathbf{H}_{\text{BP}}(z) \times \mathbf{H}_{\text{BP}}(z)$ at sampling rate $Q = 5$ kHz, center frequency $f_0 = 50$ Hz and passband $f_r - f_l = 4$ Hz

When the $\mathbf{H}_{\text{BP}}(z)$ filter (Eq. 2) is applied twice in opposite directions, the frequency response is the same. The phase response has a value of zero, therefore, when the PLI frequency deviates, no additional phase distortions occur. The double application of the BP filter in one direction is performed with Eq. (3) and (4):

% first band-pass filtration

$$\mathbf{B1}(i) = a_1 * \mathbf{B1}(i-1) - a_2 * \mathbf{B1}(i-2) + (\mathbf{mI}x(i) - \mathbf{mI}x(i-2)) * (1-a_2) / 2; \quad (3)$$

% second band-pass filtration

$$\mathbf{B2}(i) = a_1 * \mathbf{B2}(i-1) - a_2 * \mathbf{B2}(i-2) + (\mathbf{B1}(i) - \mathbf{B1}(i-2)) * (1-a_2) / 2; \quad (4)$$

where $\mathbf{mI}x$ is the contaminated ECG signal; $\mathbf{B1}$ and $\mathbf{B2}$ are the 1st harmonic PLI samples after first and the second BP filtration, respectively.

The applied second filtration (Eq. (4)) contributes to a more accurate extraction of the 1st harmonic of the PLI component from the contaminated ECG signal. Fig. 3 shows the extracted interference after stages ‘i’ and ‘ii’ (central frequency $f_0 = 50$ Hz – experiment shown in Fig. 10D). The PLI component has an added 10% 3rd harmonic, which is evident by the plateau at the top of the sinusoid (the signal in black). During the first ($\mathbf{B1}$) and second ($\mathbf{B2}$) BP filtrations, only the first harmonic of the PLI is extracted. A phase shift appears due to the nonlinear phase response of the $\mathbf{H}_{\text{BP}}(z)$ filter. The phase lags at $f_i < f_0$ (first subplot) and advances at $f_i > f_0$ (second subplot). In both cases, there is a decrease in the amplitude of the extracted 1st harmonic.

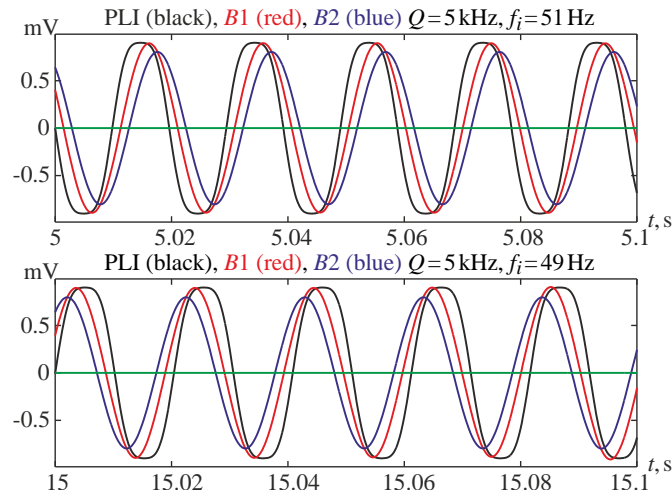


Fig. 3 Extracted 1st harmonic of PLI after stages “i” and “ii” (experiment shown in Fig. 10D)

Stage ‘iii’ – determination of coefficients for notch filtration

When replacing bidirectional filtration with unidirectional one, the problems of compensation the frequency and amplitude changes of PLI must be solved. This is done in stage “iii”, by determining the ongoing frequency f_i and coefficients $A_{1(i)}$ and $K_{B(i)}$, used for NF filtration in stage “iv” and the modified stage “v”.

Compensation of PLI frequency deviations

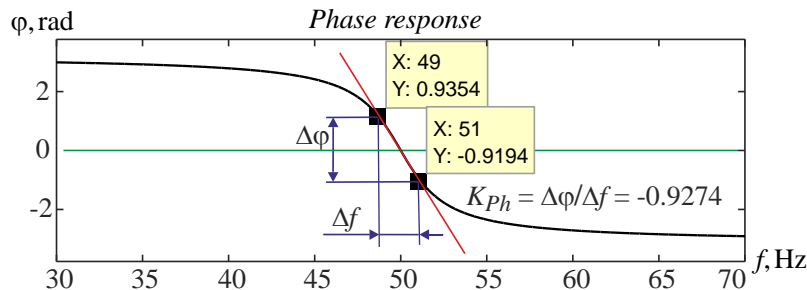


Fig. 4 Zoomed phase response of BP filter $\mathbf{H_{PB}(z)} \times \mathbf{H_{PB}(z)}$ from Fig. 2 (second subplot) in the field of $f_0 = 50$ Hz

When the PLI frequency deviates, an additional component Δf appears in the calculated from Eq. (1) ongoing frequency f_i , which generates an additional phase shift due to the nonlinear phase response of BP filtrations $\mathbf{H_{PB}(z)} \times \mathbf{H_{PB}(z)}$ (Fig. 4). The additional phase shift

$$Phs = \frac{\Delta\varphi}{\Delta t} = \frac{\Delta f}{\Delta t} K_{Ph}$$

is the first derivative of the phase response for the ongoing frequency f_i . For example, in the range of PLI frequency deviation $f_i \equiv X$ [49 ... 50 ... 51] Hz, the K_{Ph} coefficient varies in the range $K_{Ph} \equiv Y$ [-0.81 ... -1.00 ... -0.79], middle value -0.93. To increase the filtration accuracy, K_{Ph} is defined at several points (optimally 9) of the phase response in the interval of the expected PLI frequency deviation. For the purpose was used the MATLAB function `phasez()`, which calculates the phase response from the transfer function $\mathbf{H_{PB}(z)} \times \mathbf{H_{PB}(z)}$.

If it is assumed that for an interval $\Delta t = Dt$ the frequency f_i varies linearly, the additional phase

shift can be written as

$$Phs = \frac{\Delta f}{\Delta t} K_{Ph} = \frac{f_i - f_{i-Dt}}{t_i - t_{i-Dt}} K_{Ph}. \quad (5)$$

The calculated phase correction Phs is involved into the coefficient $A_{1(i)}$

$$A_{1(i)} = \frac{2}{1+k_1} \cos\left(\frac{2\pi f_i}{Q} - Phs\right), \quad k_1 = \text{tg} \frac{\pi(f_r - f_\ell)}{2Q}, \quad (6)$$

which is used in the NF filtration in stage ‘iv’ and replaces the coefficient a_1 from (Eq. (2)) in the modified NF filtration in stage ‘v’.

Fig. 5 shows the effect of introducing the phase correction into the coefficient $A_{1(i)}$ during the experiment in Fig. 10B, where the PLI frequency deviates from 61 to 59 Hz, and the amplitude from 1 to 0 mV for 20 s. The green line shows the reference coefficient $A_{1(i)}$, the blue line – the coefficient without phase correction, and the red line – the coefficient after the phase correction. The green and red lines overlap completely except for the first second, which proves the efficiency of the correction.

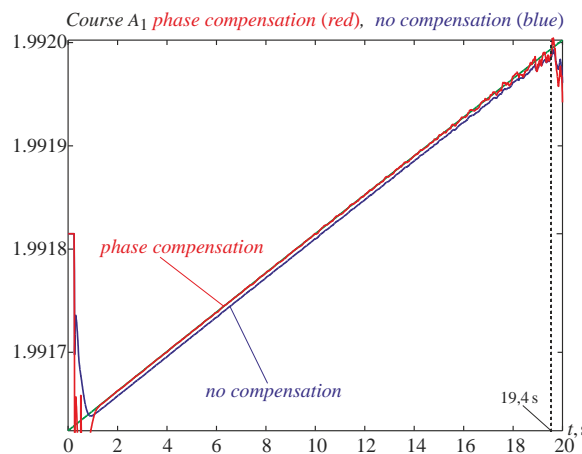


Fig. 5 Trend of the coefficient $A_{1(i)}$ with a linear deviation of the PLI frequency from 49 to 51 Hz for 20 s, at a sampling rate of 5 kHz

One may observe that after second 19.4 (at a PLI amplitude of about 30 μV) there are noticeable deviations of the coefficient $A_{1(i)}$ from the reference one. This can be considered to be the level of mains interference below which the PLI sinusoid length determination procedure should not be applied due to the generation of unrealistic values of $A_{1(i)}$. Therefore, before calculating Eq. (6), restrictions are applied

$$f_{\min} \leq f_i \leq f_{\max}, \quad \begin{cases} f_{\max} = f_0 + \frac{Df}{2} \\ f_{\min} = f_0 - \frac{Df}{2} \end{cases}, \quad (7)$$

by which the NF filtration in stages ‘iv’ and ‘v’ is maintained within the expected deviation of the PLI. Df is the range of expected PLI deviations. Additionally, a low-pass filtration is performed of $A_{1(i)}$ with a cut-off of 0.5 Hz to avoid random fluctuations.

Compensation of PLI amplitude variation

The amplitude variation of PLI causes an additional error when applying unidirectional NF filtration. In bidirectional NF filtration, such an error is compensated, since the direction of the PLI amplitude variation is opposite for the two NF filtration, successively applied in the “forward” and “backward” directions. To eliminate errors from a linearly varying PLI amplitude, a modification of the second unidirectional NF filtration was performed in stage ‘v’. For the purpose a correction factor $K_{B(i)}$ is introduced to amplify the extracted PLI, according to the relative variation in the amplitude AB of the mains interference. Fig. 6 illustrates the determination of the PLI amplitude. It is calculated by the difference between the two samples $B2_i$ and $B2_{i-1}$ on both sides of the zero line.

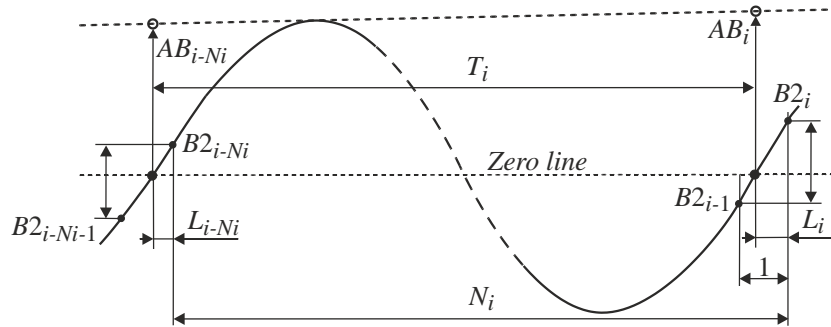


Fig. 6 Principle of compensating the PLI amplitude variation

$$\begin{cases} B2_i = AB_i \sin \frac{2\pi L_i}{T_i} K_A \\ B2_{i-1} = -AB_i \sin \frac{2\pi(1-L_i)}{T_i} K_A \end{cases} \Rightarrow AB_i = \frac{B2_i - B2_{i-1}}{\sin \frac{2\pi L_i}{T_i} + \sin \frac{2\pi(1-L_i)}{T_i}} \frac{1}{K_A} \quad (8)$$

K_A is the transfer coefficient of the BP filtration $\mathbf{H}_{PB}(z) \times \mathbf{H}_{PB}(z)$ in stages ‘i’ and ‘ii’ (Fig. 2, first subplot, and Fig. 7). As can be seen in Fig. 3, the amplitude of the extracted PLI decreases with deviation of the ongoing frequency f_i from f_0 . For example, in the range of PLI frequency deviation $f_i \equiv X$ [49...50...51] Hz the coefficient K_A varies within the limits of $K_A \equiv Y$ [0.7967...1...0.8031] (Fig. 7). To achieve high accuracy, K_A is determined at 80 points of the expected PLI frequency deviations using the MATLAB function `freqz()`, which calculates the frequency response from the transfer function $\mathbf{H}_{PB}(z) \times \mathbf{H}_{PB}(z)$.

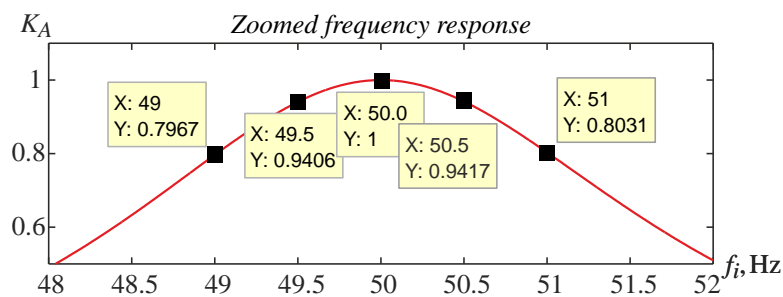


Fig. 7 Zoomed frequency response of the BP filtration $\mathbf{H}_{PB}(z) \times \mathbf{H}_{PB}(z)$ from Fig. 2 (first subplot) within the limits from $f_l = 48$ Hz to $f_r = 52$ Hz

The average relative variation of the PLI amplitude is represented by the equation:

$$RA_i = \frac{2(AB_i - AB_{i-N_i})}{AB_i + AB_{i-N_i}}. \quad (9)$$

To avoid sudden fluctuations in RA_i , an additional low-pass filtration with cut-off at 0.5 Hz is applied. The correction amplify factor $K_{B(i)}$ for PLI amplification in the modified second unidirectional NF filtration in stage 'v' is defined by

$$K_{B(i)} = 1 + RA_i \cdot K_R, \quad (10)$$

where the multiplier K_R is experimentally determined as 7.9 for $f_0 = 50$ Hz and 9.57 for $f_0 = 60$ Hz.

Procedure adaptation to low sampling rates.

The individual length of each sine wave T_i in [6] and [18] is determined by two sequential increasing crossings with the zero line. The relations L_i and L_{i+1} (1) used for this purpose represent a linear interpolation of parts of the sinusoid between their zero crossing points and the next them PLI samples. At an ECG sampling rate above 1 kHz, the linear interpolation represents quite accurately the length of parts of the sinusoid. At a lower sampling rate, a significant error occurs. To eliminate this error, a sinusoidal approximation of the intersection points is applied. The samples B_{2i} and B_{2i-1} are expressed by $B_{2i} = AB_i \sin \frac{2\pi L_i}{T_i} K_A$ and

$B_{2i-1} = -AB_i \sin \frac{2\pi(1-L_i)}{T_i} K_A$ (Fig. 6). Then the real value of L_i is determined as follows:

$$B_{rel} = \frac{B_{2i}}{B_{2i} - B_{2i-1}} = \frac{\sin \frac{2\pi L_i}{T_i}}{\sin \frac{2\pi L_i}{T_i} + \sin \frac{2\pi(1-L_i)}{T_i}}. \quad (11)$$

The calculation of L_i , as a function of B_{rel} , was performed using the successive approximation method. Fig. 8 shows the errors $Error = B_{rel} - L_i$ that occur using linear approximation of the crossing points between the PLI sinusoid and the zero line. When using a sinusoidal approximation of the intersection points, the values of L_i in Eq. (8) must be determined by Eq. (11).

Stages 'iv' and 'v' – notch (band-stop) filtration

The first NF filtration is performed in stage 'iv' using Eq. (12) just as in [6], but with values of A_1 determined by the variables f_i and Phs .

% first notch filtration 1-st harmonic

$$\mathbf{NFf}(i) = A_1(i) * \mathbf{NFf}(i-1) - A_2 * \mathbf{NFf}(i-2) - A_1(i) * \mathbf{mI\mathbf{x}}(i-1) + (1+A_2) / 2 * (\mathbf{mI\mathbf{x}}(i) + \mathbf{mI\mathbf{x}}(i-2)), \quad (12)$$

where \mathbf{NFf} is the filtered ECG signal; $\mathbf{mI\mathbf{x}}$ is the contaminated ECG signal.

$$\mathbf{H}_{\mathbf{NF}}(z) = \frac{\left(\frac{1+A_2}{2}\right) \cdot z^0 - A_1(i) \cdot z^{-1} + \left(\frac{1+A_2}{2}\right) \cdot z^{-2}}{1 - A_1(i) \cdot z^{-1} + A_2 \cdot z^{-2}}, \quad \left| \begin{array}{l} A_1(i) = \frac{2}{1+k_1} \cdot \cos\left(\frac{2 \cdot \pi \cdot f_i}{Q} - Phs\right), \\ A_2 = \frac{1-k_1}{1+k_1}, \quad k_1 = \text{tg} \frac{\pi \cdot (f_r - f_\ell)}{2 \cdot Q} \end{array} \right. \quad (13)$$

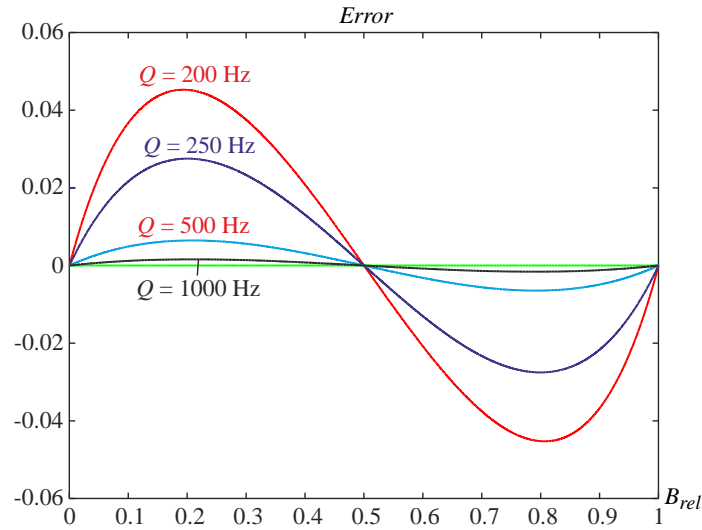


Fig. 8 Errors in linear approximation of the crossing point between the PLI sinusoid and the zero line for different sampling frequencies Q

The filter (Eq. (13)) is used, with the calculated ongoing frequency f_i (1) and $A_{1(i)}$ (Eqs. (6), (7)). A twice narrower band-stop $(f_r - f_d)/2$ is applied, which is reflected on the coefficient k_1 .

The modified NF filtration in stage ‘v’ is performed in the following sequence:

- The PLI from stage ‘iv’ is extracted and amplified by a factor $K_{B(i)}$ (Eq. (14));
- A third BP filtration with the same amplify factor is applied (Eq. (15)) using the BP filter (Eq. (2)), where the coefficients a_1 and a_2 are replaced by $A_{1(i)}$ and A_2 (Eq. (13)), respectively.
- The filtered and amplified PLI 1st harmonic is extracted from the contaminated signal (Eq. (16)).

% modified second notch filtration 1-st harmonic

$$\mathbf{B3}(i) = (\mathbf{mI}x(i) - \mathbf{NF}f(i)) * \mathbf{KB}(i) \quad (14)$$

$$\mathbf{B}(i) = \mathbf{A1}(i) * \mathbf{B}(i-1) - \mathbf{A2} * \mathbf{B}(i-2) + (\mathbf{B3}(i) - \mathbf{B3}(i-2)) * (1 - \mathbf{A2}) / 2 * \mathbf{KB}(i) \quad (15)$$

$$\mathbf{NF}(i) = \mathbf{mI}x(i) - \mathbf{B}(i) \quad (16)$$

where \mathbf{NF} is the filtered ECG signal; $\mathbf{mI}x$ is the contaminated ECG signal; $\mathbf{NF}f$ is the filtered ECG signal after stage ‘iv’; $\mathbf{B3}$ and \mathbf{B} are the 1st harmonic PLI samples amplified after Eq. (14) and Eq. (15), respectively; $\mathbf{KB}(i) \equiv K_{B(i)}$ is the amplify factor.

Fig. 9 shows the results from the experiment presented in Fig. 10C: the twice-amplified after Eq. (15) PLI (first subplot) and the variable amplify factor $K_{B(i)}$ (second subplot). Both, subplots contain the determined amplitude of the mains interference.

Elimination of high-order harmonics in the power-line interference

According to European and Bulgarian standards, the main high-order harmonics presented in the supply voltage of public distribution systems are 3rd $\leq 5\%$, 5th $\leq 6\%$, 7th $\leq 5\%$, 11th $\leq 3.5\%$ and 13th $\leq 3\%$, with an acceptable total harmonic distortion (THD) $\leq 8\%$ [12].

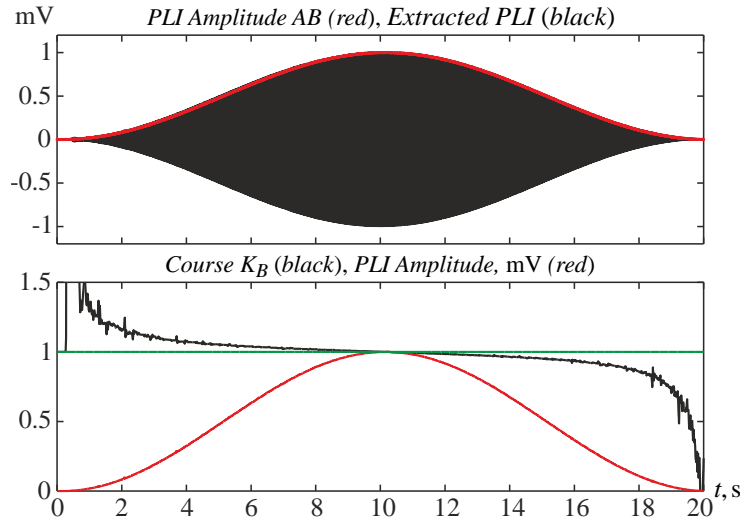


Fig. 9 Illustration of stages 'iv' and 'v'

In the present work, each of the high-order PLI harmonics is removed independently by a single NF filtration (Eq. (13)), where the coefficients $A_{1(i)}$ and A_2 are replaced by $A_{N(i)}$ and A_{2N} , respectively

$$\left| \begin{aligned} A_{N(i)} &= \frac{2}{1+k_N} \cos\left(\frac{2\pi N f_i}{Q} - NPhs\right), & k_N &= \text{tg} \frac{\pi N(f_r - f_l)}{4Q}, \\ A_{2N} &= \frac{2}{1+k_N} \end{aligned} \right. \quad (17)$$

where N is the number of the high-order PLI harmonic. The stop-band is reduced twice compared to that of $A_{1(i)}$. Additionally, a low-pass filtration of $A_{N(i)}$ is needed.

Experiments and results

The test of the filtration procedure is carried out using conditionally clean recordings taken from the AHA database which then are resampled with different sampling rates and additionally mixed by synthesized PLI. The interference has a frequency of 50 or 60 Hz, which deviates within the limits of ± 1 Hz for 20 s and an amplitude varying from 0 to 1 mV according to linear or sinusoidal law. In some of the tests, a 3rd PLI harmonic is added with amplitude representing 10 % of that of the 1st harmonic. The results obtained are evaluated by the error ErrMax representing the maximum absolute difference between mixed and filtered ECG signals, as well as by the traditional for other studies root mean square error (RMS). The edges of the signals are excluded from the evaluation. Each of the experiments is illustrated by three subplots – the first contains the contaminated signal, the second one shows the filtered signal, and the third illustrates the difference between original and filtered signal.

Fig. 10 shows the results of experiments with the AHA1003 signal, resampled at 5 kHz. The pilot experiment A is performed with a clean signal in order to evaluate the procedure in absence of PLI. For the other cases, the added PLI has a center frequency of 50 Hz, linearly deviating from 49 to 50 Hz for 20 s. In B, the PLI amplitude linearly varies from 0 to 1 mV. In C and D, a 3rd PLI harmonic is added. The PLI amplitude in C varies according to a sinusoidal law. In D, an abrupt change of the PLI frequency from 51 to 49 Hz is introduced in the middle of the recording to evaluate the set-up time of the procedure.

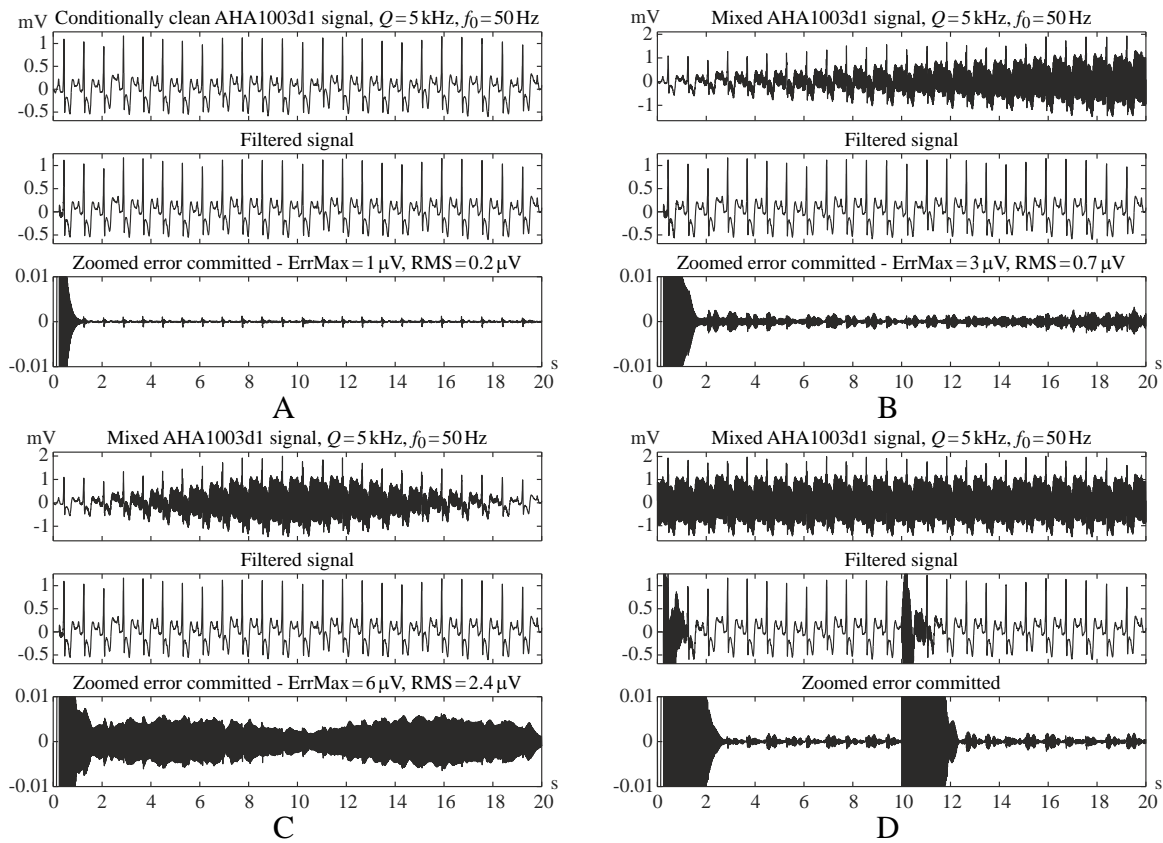


Fig. 10 Experiments with the AHA1003 ECG signal

Fig. 11 demonstrates the results of experiments with the AHA1005 signal, resampled at 5 kHz. A PLI with a frequency of 60 Hz, deviating linearly from 61 to 59 Hz and a 3rd PLI harmonic is added (Experiment A). Experiment B has linearly varying PLI amplitude from 1 to 0 mV within 20 s.

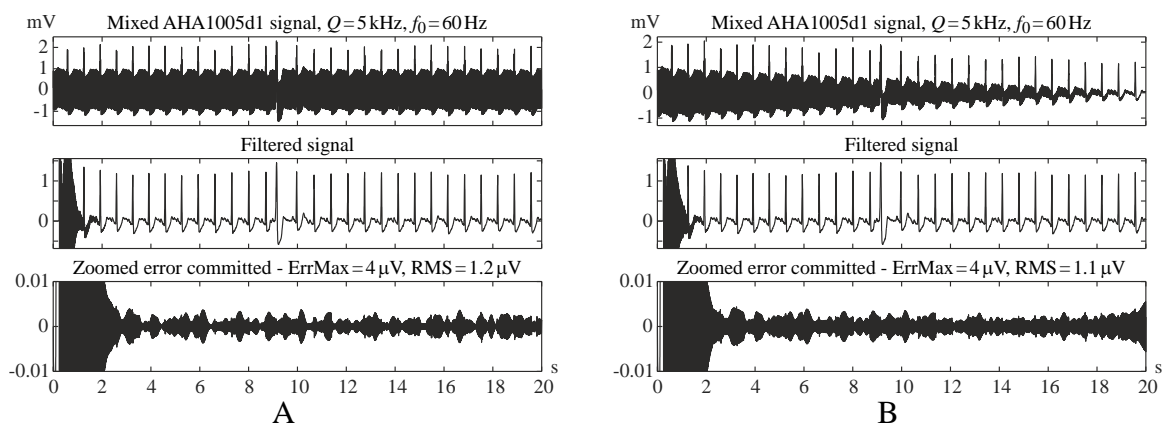


Fig. 11 Experiments with the AHA1005 ECG signal

The following experiments are carried out at low sampling rates. Fig. 12 illustrates experiments with the AHA7009 signal resampled at 500 Hz. Here a ± 1 Hz PLI with center frequency of 50 Hz for experiment A and 60 Hz for experiment B is added together with a 3rd PLI harmonic. Experiment A has a linearly varying PLI amplitude from 1 to 0 mV for 20 s.

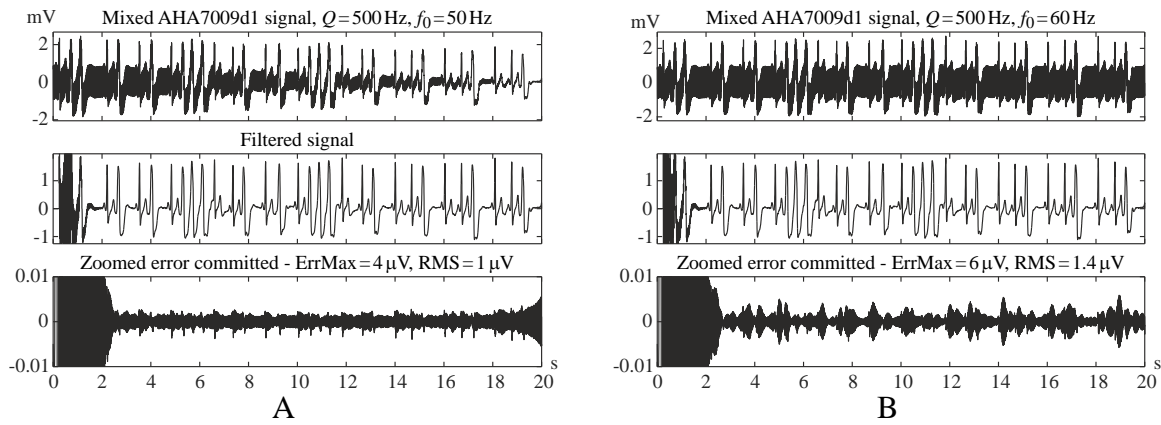


Fig. 12 Experiments with the AHA7009 ECG signal

Fig. 13 demonstrates two experiments with the AHA1001 signal, sampled at 250 Hz. Here a ± 1 Hz PLI for 20 s with center frequency of 50 Hz for A and 60 Hz for B is added.

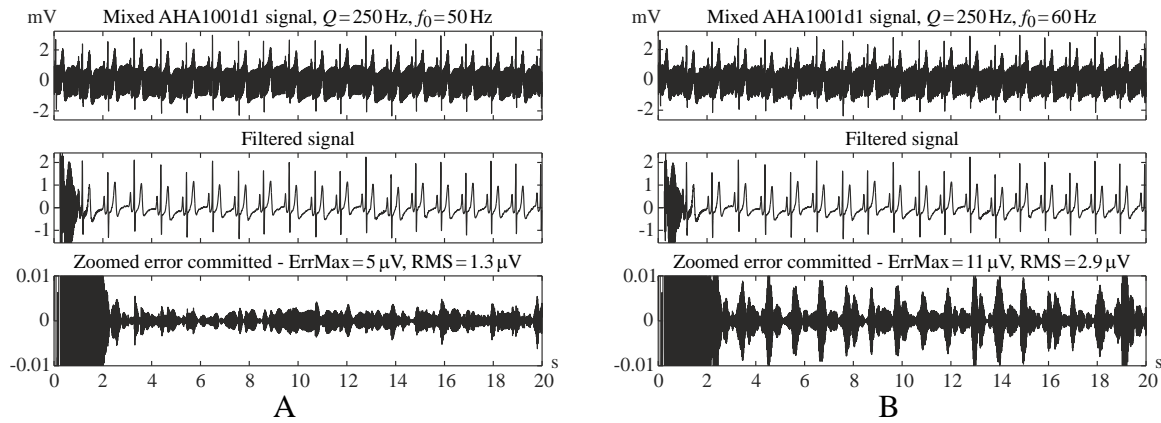


Fig. 13 Experiments with the AHA1001 ECG signal

Table 1 demonstrates experimental results of PLI elimination (ErrMax and RMS errors) obtained by identical tests performed using the elaborated and discussed in this paper ‘Real time’ version, as well as the previously published ‘Bidirectional’ [6] and ‘Quasi-real time’ [18] versions. The main criterion of the ECG signals filtration is the absolute maximum error ErrMax, since it has a very strong negative impact on the morphological analysis of ECG signals based on time-amplitude criteria. Although RMS does not assess adequately the compromised ECG signals, this error is calculated because many authors use it as an additional indicator in linear filtration procedures.

The analysis of the results in Table 1 shows the following:

- The errors obtained at high sampling rates (Figs. 10, 11) are identical for the three versions of the procedure;
- The higher errors at low sampling rates (Figs. 12, 13) committed by the ‘Bidirectional’ version [6] are due to the use of linear interpolation of the PLI sinusoid crossing points instead of the sinusoidal one;
- The damaged filtration at low sampling rates (Figs. 12, 13) obtained by the ‘Quasi-real time’ version [18] are due to the insufficient overlap time in the NF filtration in stage ‘v’.

Table 1. Results of tests with different versions of the filtration procedure

Experiment	‘Real time’		‘Bidirectional’ [6]		‘Quasi-real time’ [20]	
	ErrMax, μV	RMS, μV	ErrMax, μV	RMS, μV	ErrMax, μV	RMS, μV
Fig. 10A	1	0.2	2	0.3	2	0.3
Fig. 10B	3	0.7	2	0.4	2	0.5
Fig. 10C	6	2.4	4	1.6	6	1.7
Fig. 10D	setup time 2.3 s		setup time 1.6 s		setup time 1.6 s	
Fig. 11A	4	1.2	3	0.4	3	0.4
Fig. 11B	4	1.1	3	0.7	4	0.8
Fig. 12A	4	1.0	12	1.5	does not operate	
Fig. 12B	6	1.4	18	1.8	does not operate	
Fig. 13A	5	1.2	32	12.9	does not operate	
Fig. 13B	10	2.7	71	30.2	does not operate	

A comparison between the three NF versions – ‘Bidirectional’, ‘Quasi real time’ and ‘Real time’, suggests their areas of application. The first one is the simplest because the bidirectional BP and NF filtrations automatically compensate both amplitude and frequency PLI deviations regardless of their direction. However, this version cannot operate in real time mode, which makes it applicable only for offline ECG signals processing, e.g., in Holter recordings. The ‘Real time’ version achieves identical results as the ‘Bidirectional’ one, but at the expense of highly complicated additional calculations for compensating the PLI frequency and amplitude changes. This explains the slightly larger errors (about 1 – 2 μV) compared to the ‘Bidirectional’ version. The ‘Real time’ version is suitable for online processing, for example when monitoring ECG signals. The ‘Quasi-real time’ version compensates PLI amplitude and frequency changes both in online and offline procedures, but only at high sampling rates of the ECG signals.

Conclusions and discussion

This paper manifests a procedure for almost complete elimination of PLI using modified notch filtering. The procedure uses the sequence of filtration stages introduced in [6] by replacing the BP filtration “backward” in stage ‘ii’ by a second BP filtration “forward” and the NF filtration “backward” in stage ‘v’ by a modified NF filtration “forward”.

Stages ‘i’ and ‘ii’ apply the same filter (Eq. (2)) and could be combined into one stage – the result will be identical. Due to the use of a constant coefficient a_1 , a phase shift occurs in the extracted first harmonic of the mains interference. However, it is the same for the beginning and the end of the ongoing PLI sinusoid (Fig. (3)) and does not interfere with the determination of ongoing frequency f_i . The calculated ongoing coefficients $A_{N(i)}$ (Eqs. (6), (17)) change the notch and BP filters used in stages ‘iv’ and ‘v’ so that for the ongoing frequency f_i their phase response has values of zero.

The manifested procedure is adapted to a deviation in the PLI frequency by the introduced phase correction Phs (Eqs. (5), (6), (17)). Adaptation to a PLI amplitude variation has been successfully performed by means of the additionally introduced gain coefficient $K_{B(i)}$ in the modified notch filter (Eqs. (14), (15)). The adaptation is performed under the assumption that the changes in PLI are linear in the interval $Dt \approx 125$ ms. The coefficients K_{Ph} and K_A used for

Phs (Eq. (5)) and K_B (Eq. (8)) are calculated in the range from 49 to 51 Hz with MATLAB functions and saved in advance in arrays, thus not introducing a delay in the execution of the procedure.

The proposed sinusoidal approximation of the PLI sinusoid crossing points with the zero line allows the application of the procedure at low sampling rates of the ECG signal. Due to the introduced limitation for maximum and minimum values of the ongoing frequency f_i , the NF filtration does not involve distortions into the filtered ECG signal in the absence of mains interference (see the pilot experiment in Fig. 10A).

Some noted features:

- There is an increase of the error in case of a nonlinear variation in the PLI amplitude;
- Identical experiments performed with PLI 60 Hz, (Fig. 10B, Fig. 12A and Fig. 13A) and PLI 50 Hz (Fig. 11B, Fig. 12B and Fig. 13B) show twice larger error for the first case the resulted error is about twice as large as in the corresponding ones;
- The experimental determination of the multiplier K_R (Eq. (10)) cannot be theoretically explained.

References

1. Badreldin I. S., D. S. El-Kholy, A. A. Elwakil (2012). Harmonic Adaptive Noise Canceler for Electrocardiography with No Power-line Reference, 16th IEEE Mediterranean Electrotechnical Conference, 1017-1020.
2. Dobrev D., T. Neycheva, N. Mudrov (2008). Digital Lock-in Techniques for Adaptive Power-line Interference Extraction, *Physiological Measurement*, 29(7), 803.
3. Dobrev D., T. Neycheva, V. Krasteva, I. Iliev (2010). High-Q Comb FIR Filter for Mains Interference Elimination, *Annual Journal Electronics*, 4(2), 126-129.
4. Dotsinsky I. (2005). Removal of Frequency Fluctuating Power-line Interference from ECG. 3rd European Medical & Biological Engineering Conference EMBEC'05, Prague, Czech Republic IFMBE Proceedings, 2005, 11(1), 4752-4755.
5. Dotsinsky I. (2005). Suppression of AC Railway Power-line Interference in ECG Signals Recorded by Public Access Defibrillators, *BioMedical Engineering OnLine*, 4(1), 65.
6. Dotsinsky I. (2022). An Approach to Successful Power-line Interference Suppression in ECG Signals, *International Journal Bioautomation*, 26(1), 83-92.
7. Dotsinsky I., T. Stoyanov (2005). Power-line Interference Cancellation in ECG Signals, *Biomedical Instrumentation & Technology*, 39(2), 155-162.
8. Dotsinsky I., T. Stoyanov (2008). Power-line Interference Removal from ECG in Case of Power-line Frequency Variations, *International Journal Bioautomation*, 10, 88-96.
9. Dotsinsky I., T. Stoyanov, G. Mihov (2020). Power-line Interference Removal from High Sampled ECG Signals Using Modified Version of the Subtraction Procedure, *International Journal Bioautomation*, 24(4), 381-392.
10. Ivanov K., I. Jekova, V. Krasteva (2023). Convolutional Autoencoder for Filtering of Power-line Interference with Variable Amplitude and Frequency: Study of 12-lead PTBXL ECG Database, *International Symposium on Bioinformatics and Biomedicine*, 121-133.
11. Levkov C., G. Mihov, R. Ivanov, I. Daskalov, et al. (2005). Removal of Power-line Interference from the ECG: A Review of the Subtraction Procedure, *Biomedical Engineering Online*, 4(1), 50.
12. Markiewicz H., K. Antony (2004). Standard EN 50160 – Voltage Characteristics of Public Distribution Systems, Wroclaw University of Technology, Power Quality Blog, <https://powerquality.blog/2021/07/22/> (access date 09 February 2026).

13. Mateo J., C. Sánchez, A. Torres, R. Cervigon, et al. (2008). Neural Network Based Cancellor for Powerline Interference in ECG Signals, *Computers in Cardiology*, 35, 1073-1076.
14. Neycheva T., D. Dobrev, N. Mudrov (2009). High-Q Bandpass Comb Filter for Mains Interference Extraction, *International Journal Bioautomation*, 13(4), 7-12.
15. Razzaq N., S. Sheikh, M. Salman, T. Zaidi (2016). An Intelligent Adaptive Filter for Elimination of Power Line Interference from High Resolution Electrocardiogram, *IEEE Access*, 4, 1676-1688.
16. Rizanov S., G. Mihov (2025). Genetic Filtering of Power-line Interference in Electrocardiograms, 34-th International Scientific Conference Electronics, 1-6.
17. Shaddeli R., N. Yazdanjue, S. Ebadollahi, M. M. Saberi, et al. (2021). Noise Removal from ECG Signals by Adaptive Filter Based on Variable Step Size LMS Using Evolutionary Algorithms, *IEEE Canadian Conference on Electrical and Computer Engineering*, 1-7.
18. Stoyanov T., I. Dotsinsky, G. Mihov (2024). Power-line Interference Elimination from ECG Signals Using Notch Filtration: A Quasi-real Time Version, *International Journal Bioautomation*, 28(3), 161-170.
19. Stoyanov, T., I. Christov, I. Jekova, V. Krasteva (2010). Online Adaptive Filter for Mains Interference Suppression in Diagnostic Electrocardiographs: Cases of Amplitude and Frequency Deviation, *Annual Journal Electronics*, 4, 150-153.
20. Ur-Rehman I., H. Raza, N. Razzaq, T. Zaidi (2021). Parallel Distributed Framework for State Space Adaptive Filter for Removal of PLI from Cardiac Signals, *International Journal Bioautomation*, 25(3), 249-270.

Prof. Georgy Mihov, D.Sc.

E-mail: gsm@tu-sofia.bg



Georgy Mihov obtained his M.Sc. Degree from the Faculty of Radioelectronics, Technical University of Sofia. In 2013 he obtained D.Sc. Degree on the Subtraction Procedure for Interferences Removal from ECG. Since 2007 G. Mihov is a Professor with the Technical University of Sofia. His interests are mainly in the field of digital electronics, digital filtration, microprocessor system applications and servicing. He is a Corresponding Member of the Bulgarian Academy of Sciences since 2018.

Prof. Ivan Dotsinsky, D.Sc.

E-mail: iadoc34@gmail.com



Ivan Dotsinsky obtained his M.Sc. Degree from the Faculty of Electrical Engineering, Technical University of Sofia. In 1987 he obtained the Dr. Eng. Sc. Degree on Instrumentation of Electrocardiology. Since 1989, he has been a Professor in Biomedical Engineering. Since 1994, he is a Professor with the Centre of Biomedical Engineering and the Institute of Biophysics and the Institute of Biophysics and Biomedical Engineering Bulgarian Academy of Sciences. Prof. Dotsinsky's interests are mainly in the field of acquisition, preprocessing, analysis and recording of biomedical signals.



© 2026 by the authors. Licensee Institute of Biophysics and Biomedical Engineering, Bulgarian Academy of Sciences. This article is an open access article distributed under the terms and conditions of the Creative Commons Attribution (CC BY) license (<http://creativecommons.org/licenses/by/4.0/>).